

# Self-consistent ballistic and diffusive spin transport across interfacial resistances in a hybrid ferromagnet-semiconductor trilayer

S. Agrawal,<sup>1</sup> M. B. A. Jalil,<sup>1</sup> S. G. Tan,<sup>2</sup> K. L. Teo,<sup>1</sup> and T. Liew<sup>1,2</sup>

<sup>1</sup>Information Storage Materials Laboratory, Department of Electrical and Computer Engineering, National University of Singapore, 4 Engineering Drive 3, Singapore 117576, Singapore

<sup>2</sup>Data Storage Institute, DSI Building, 5 Engineering Drive 1 (Off Kent Ridge Crescent), National University of Singapore, Singapore 117608, Singapore

(Received 23 March 2005; revised manuscript received 28 June 2005; published 22 August 2005)

Spin dependent interfacial resistance ( $R_I$ ) is crucial for achieving high spin injection efficiency from a ferromagnetic (FM) metal into a semiconductor (SC). We present a self-consistent model of spin transport across interfacial resistances at the FM–SC junctions of a FM–SC–FM trilayer structure. The SC layer consists of a highly doped  $n^{++}$  AlGaAs—GaAs 2DEG while the interfacial resistance at the FM–SC junction is modeled as delta potential ( $\delta$ ) barriers. The self-consistent scheme consists of a ballistic model of spin-dependent transmission across the  $\delta$  barriers to evaluate  $R_I$ , and a drift-diffusion model to obtain the spin-split  $\Delta\mu$  in the electrochemical potentials. The  $R_I$  values of the two junctions were found to be asymmetric despite the symmetry of the trilayer structure. This asymmetry arises from the finite biasing voltage which causes a difference in electrochemical potentials and spin accumulation at the two interfaces. The effect of  $R_I$  on the spin-injection efficiency and magnetoresistance is studied over a range of  $\delta$ -barrier heights. Significant spin-injection efficiency (50%) requires high  $\delta$ -barrier heights approaching 1 eV. Even higher barrier heights are required to obtain equivalent magnetoresistive effect.

DOI: [10.1103/PhysRevB.72.075352](https://doi.org/10.1103/PhysRevB.72.075352)

PACS number(s): 73.40.Cg, 73.40.Sx, 72.25.Mk

## I. INTRODUCTION

Semiconductor (SC)-based spintronics<sup>1</sup> which exploits the spin as well as the charge property of carriers, is a fast growing field of research. The long spin coherence of electrons in SC,<sup>2</sup> coupled with the ability to control spin orientation by electrical means<sup>3</sup> has opened the possibility of realizing devices such as the Datta–Das spin field effect transistor<sup>4</sup> (spin-FET). A chief prerequisite of such devices is the ability to inject spin-polarized current into the semiconductor material, which are usually nonmagnetic. Early experimental efforts at spin injection were not very successful with spin injection efficiency  $\eta$  of the order of 1% only.<sup>5,6</sup> More recent attempts, however, have achieved reasonably high injection efficiency  $\eta$  exceeding 30%.<sup>7</sup> The crucial element for their success is the incorporation of interfacial barriers, e.g., tunnel or Schottky barriers between the FM and SC layers.

Thus, the main focus of this article is to investigate the effect of the interfacial resistances ( $R_I$ ) at the FM–SC boundary on the spin injection efficiency and overall magnetoresistance of a FM–SC–FM trilayer. Our model is based on the spin-dependent drift-diffusion (DD) equation. Previously, van Son *et al.*<sup>8</sup> applied the DD equation in the case of a single FM–NM junction with a finite  $R_I$ . His calculations yield a split in the electrochemical potential  $\mu$  for carriers of minority and majority spin directions, as well as a discontinuity of the potentials  $\Delta\mu$  at the interface due to  $R_I$ . Subsequently, Schmidt *et al.*<sup>9</sup> applied the DD model to a trilayer structure. They found that in the absence of  $R_I$ , the resultant spin injection efficiency  $\eta$  and magnetoresistance are heavily suppressed due to the conductivity mismatch between the metallic FM and the SC layers. This accounts for the low  $\eta$  of the device by Hammar *et al.*<sup>5</sup> Rashba<sup>10</sup> proposed a solu-

tion to this problem, by incorporating a tunnel barrier. However, in Rashba’s model, the interfacial resistances are assigned arbitrary values, and these are taken to be identical for the left and right interfaces for a symmetric FM–NM–FM trilayer (i.e., identical FM material). Similar assumptions are also made by Yu and Flatté<sup>11</sup> in applying the DD model to a FM/NM/FM trilayer.

In our model, these assumptions are removed, and instead the  $R_I$  values are obtained self-consistently with the diffusive spin transport in the bulk FM and SC layers. The  $R_I$  values are evaluated by considering ballistic tunneling transmission across  $\delta$ -function potential barriers at the FM–SC interfaces. The incorporation of interfacial  $\delta$  barriers makes our model similar to that of Heershe *et al.*,<sup>12</sup> but the latter assumes fully ballistic transport through the structure and is limited to a single junction. Similarly, Tao *et al.*<sup>13</sup> have also done a fully ballistic analysis of spin transport in a FM/SC/FM double tunnel junction based on a quantum statistical approach. Their model does not take into account the diffusion equation and Ohm’s law, both of which describes the spin transport away from the interfacial zones. However in this paper, we consider a trilayer structure in which the SC layer thickness  $w$  is assumed to be larger than the carrier mean free path (MFP), although it is comparable to the spin diffusion length in the SC material. It is thus necessary to model charge transport in the SC layer away from the interfacial zones, in the diffusive regime. In our model, the overall spin current is determined self-consistently, taking into consideration the ballistic transmission through the interfacial  $\delta$  barriers and diffusive transport in the bulk of the SC and FM layers, away from the interfaces. The trilayer material consists of a highly doped  $n^{++}$  AlGaAs—GaAs 2DEG (SC) layer sandwiched between two Fe (FM) layers.

The  $\delta$ -potential barriers at the two FM–SC interfaces are expressed as  $U[\delta(x) + \delta(x-w)]$ , with the barrier height  $U$  being spin dependent, as was assumed by Yu *et al.*,<sup>11</sup> and Smith *et al.*<sup>14</sup> In fact, the quantitative description of tunneling at the FM–SC interface is rather complicated because the transport properties are strongly dependent on the potential barrier height and thickness, and are highly sensitive to interfacial roughness and impurity states within the barriers. As a first approximation, we ignore any type of electron scattering within the barriers and assume purely ballistic transport through them. It should be noted this ballistic transport analysis applies only in the vicinity of the  $\delta$ -potential barriers at the interfaces of the trilayer structure. The transport across rest of the bulk structure is governed by the DD model.

## II. MODEL

For transport in the bulk FM and SC layers, we consider the drift-diffusion model, which is based on the following equations:

$$\frac{\partial^2(\mu_{\uparrow} - \mu_{\downarrow})}{\partial x^2} = \frac{\mu_{\uparrow} - \mu_{\downarrow}}{\lambda^2}, \quad (1)$$

$$\frac{\partial \mu_{\uparrow(\downarrow)}^c}{\partial x} = \frac{e j_{\uparrow(\downarrow)}^c}{\sigma_{\uparrow(\downarrow)}^c}, \quad (2a)$$

$$\frac{\partial \mu_{\uparrow(\downarrow)}^s}{\partial x} = \frac{e j_{\uparrow(\downarrow)}^s}{\sigma_{\uparrow(\downarrow)}^s}, \quad (2b)$$

where  $\lambda$  is the spin-diffusion length and  $e$  is the magnitude of electronic charge. Subscripts  $c$  and  $s$  refers to FM contact and 2DEG SC layer.  $\mu_{\uparrow(\downarrow)}^{c,s}$ ,  $j_{\uparrow(\downarrow)}^{c,s}$ , and  $\sigma_{\uparrow(\downarrow)}^{c,s}$  are respectively, the electrochemical potentials, current densities, and conductivities for majority (minority) spin electrons, each of which are different in FM and SC 2DEG region. Equation (1) is the diffusion equation which describes the relaxation of the spin-split ( $\mu_{\uparrow} - \mu_{\downarrow}$ ), while Eqs. (2a) and (2b) are Ohm's law in FM and 2DEG regions, respectively, relating current flow to the potential gradient. In our model, we consider the conduction in a highly doped 2DEG. In such a system, it is a good approximation to assume charge neutrality, i.e., no charge accumulation. Such an approximation has been made by Zhang *et al.*<sup>15</sup> in their diffusive transport model where they have dropped the terms involving charge accumulation. Furthermore, although the electrochemical potential and charge accumulation are related by the Poisson equation, it does not matter how the two are distributed as far as transport equations are concerned, according to Stiles and Zangwill.<sup>16</sup> Thus, there is a freedom in choosing the solution of Poisson's equation and for simplicity we choose a solution corresponding to zero charge accumulation. Hence, instead of solving the diffusion equation and Poisson's equation self-consistently, we model the diffusive spin transport by solving the diffusion equation alone.

The spin diffusion length in SC can be several orders of magnitude larger than that in FM.<sup>2</sup> In the FM layer away from the interfaces at  $x=0$  and at  $x=w$ , the spin-split ( $\mu_{\uparrow}$

$-\mu_{\downarrow}$ ) tends to 0, but as the potentials approach the interfaces, an appreciable spin-splitting occurs. In contrast to FM, the SC layer has the same density of states for up-spin and down-spin electrons, so spin-splitting in electrochemical potentials is required to achieve spin polarization. We have assumed no spin-flip scattering at the interface so that  $j_{\uparrow}$  and  $j_{\downarrow}$  are continuous at the interfaces.

At the FM–SC interface, there is a discontinuity in both  $\mu_{\uparrow}$  and  $\mu_{\downarrow}$ , which is given by

$$\Delta \mu_{\uparrow,\downarrow}^{0,w} = \frac{e j_{\uparrow,\downarrow}^c}{G_{\uparrow,\downarrow}^{L,R}}, \quad (3)$$

where  $G_{\uparrow,\downarrow}^{L,R} = G_{\uparrow,\downarrow}^{L,R}/A_{\text{FM}}$  is the equivalent interfacial conductance experienced by electrons as seen from FM side with units of  $\Omega^{-1} \text{ cm}^{-2}$ ,  $A_{\text{FM}}$  is the cross-sectional area of ferromagnetic layer, and  $G_{\uparrow,\downarrow}^{L,R}$  (in units of  $\Omega^{-1}$ ) is the reciprocal of the interfacial resistance obtained through Landauer's formula (see below). We introduce  $\alpha$  and  $\beta$  as the spin polarization of current and conductivity, respectively, i.e.,  $j_{\uparrow} = \beta j$ ,  $j_{\downarrow} = (1-\beta)j$ ,  $\sigma_{\uparrow} = \alpha\sigma$ , and  $\sigma_{\downarrow} = (1-\alpha)\sigma$ , where  $j$  is the total current density.  $\beta$  is continuous across the FM–SC interfaces, because we assume no spin-flip scattering at the interfaces. As the electron density is high in the FM contact regions and is not much affected by spin accumulation, its conductivity  $\alpha_c$  there can be taken to be constant. For the SC region, we have used a 2DEG in which the Fermi level lies in the conduction band. For such a highly doped semiconductor in the metallic regime, we can to a first approximation, neglect the change in the conductivity due to the electrochemical potential difference ( $\mu_{\uparrow} - \mu_{\downarrow}$ ). Thus, based on this approximation, the conductivity in the SC is spin independent and the polarization parameter  $\alpha_s$  in the SC takes a constant value of

$$\alpha_s = \frac{\sigma_{\uparrow}}{\sigma_{\uparrow} + \sigma_{\downarrow}} = \frac{1}{2}. \quad (4)$$

The solutions to Eq. (1) for the three regions can be written as

$$(\mu_{\uparrow} - \mu_{\downarrow}) = A e^{x/\lambda_c}, \quad x < 0, \quad (5)$$

$$(\mu_{\uparrow} - \mu_{\downarrow}) = B e^{-x/\lambda_s} + C e^{-(w-x)/\lambda_s}, \quad 0 < x < w, \quad (6)$$

$$(\mu_{\uparrow} - \mu_{\downarrow}) = D e^{-(x-w)/\lambda_c}, \quad x > w. \quad (7)$$

To determine the coefficients  $A$  to  $D$ , we apply Eqs. (2a) and (2b) on both sides of the left FM-SC interface, which yields the following relations:

$$\frac{e j_c}{\sigma_c} \left[ \frac{\beta^L - \alpha_c}{\alpha_c(1 - \alpha_c)} \right] = \frac{A}{\lambda_c}, \quad (8)$$

$$\frac{e j_s}{\sigma_s} \left[ \frac{\beta^L - \alpha_s}{\alpha_s(1 - \alpha_s)} \right] = \frac{-B + C e^{-w/\lambda_s}}{\lambda_s}. \quad (9)$$

Similarly, we apply Eqs. (2a) and (2b) on both sides of the right SC-FM interface, which gives

$$\frac{e j_s}{\sigma_s} \left[ \frac{\beta^R - \alpha_s}{\alpha_s(1 - \alpha_s)} \right] = \frac{-B e^{-w/\lambda_s} + C}{\lambda_s}, \quad (10)$$

TABLE I. Parameter values assumed in numerical calculations.

$j_c$ , current density in the FM region	1 A/cm <sup>2</sup>
$\sigma_c$ , FM contact conductivity	10 <sup>6</sup> Ω <sup>-1</sup> cm <sup>-1</sup>
$A_{\text{FM}}$ , cross-sectional area of FM contact	200 nm × 200 nm (in yz plane)
$j_s$ , current density in the 2DEG region	$j_c \times 200$ nm = $2 \times 10^{-5}$ A/cm
$\sigma_s$ , 2DEG conductivity	$5.55 \times 10^{-6}$ Ω <sup>-1</sup>
$m^*$ (GaAs), effective mass of 2DEG GaAs	0.067 $m_e$ ( $m_e = 9.1 \times 10^{-31}$ kg)
$m^*$ (Fe), effective mass of Fe	1 $m_e$
$\lambda_s$ , SC spin-diffusion length	1 μm
$\lambda_c$ , contact spin-diffusion length	100 nm
$\alpha_c^L = \alpha_c^R$ , contact polarization parameter	0.7
$\delta t$ , barrier thickness	1 nm
$E_F$ (Fe), Fermi level of Fe	11.10 eV
$E_F$ (GaAs), Fermi level of GaAs 2DEG	3.5 meV
$h_0$ , molecular field	0.25 eV
$E_B$ , diff in Fermi levels of FM and 2DEG	$E_F(\text{Fe}) - E_F(2 \text{ DEG})$
$w$ , 2DEG layer width	100 nm
$h$ , Planck's constant	$6.6 \times 10^{-34}$ Js

$$\frac{ej_c}{\sigma_c} \left[ \frac{\beta^R - \alpha_c}{\alpha_c(1 - \alpha_c)} \right] = -\frac{D}{\lambda_c}. \quad (11)$$

In the above equations,  $\beta^{L,R}$  refer to the interfacial values of the spin polarization of current [i.e.,  $\beta^L = \beta(0)$ ,  $\beta^R = \beta(w)$ ]. In FM contact,  $j_c$  and  $\sigma_c$  are expressed in conventional units of A/cm<sup>2</sup> and Ω<sup>-1</sup>cm<sup>-1</sup>, respectively, while in 2DEG  $j_s$  and  $\sigma_s$  are expressed in A/cm and Ω<sup>-1</sup>, respectively, so that  $(j_c/\sigma_c)$  and  $(j_s/\sigma_s)$  have the same units. The value of  $\sigma_s$  (see Table I) is assumed to be comparable to that of Drichko *et al.*<sup>17</sup> Another set of relations between parameters  $A$ ,  $B$ ,  $C$ , and  $D$  can be obtained by applying Eq. (3) at the left and right interfaces. The discontinuity in the potential for both spin orientations, i.e.,  $\Delta\mu_{\uparrow}$ , and  $\Delta\mu_{\downarrow}$  are obtained in terms of  $G_{\uparrow(\downarrow)}$ , and subtracted from each other to yield

$$ej_c \left[ \beta^L \left( \frac{1}{G_{\uparrow\text{eq}}^L} + \frac{1}{G_{\downarrow\text{eq}}^L} \right) - \frac{1}{G_{\downarrow\text{eq}}^L} \right] = B + Ce^{-w/\lambda_s} - A, \quad (12)$$

$$ej_c \left[ \beta^R \left( \frac{1}{G_{\uparrow\text{eq}}^R} + \frac{1}{G_{\downarrow\text{eq}}^R} \right) - \frac{1}{G_{\downarrow\text{eq}}^R} \right] = D - Be^{-w/\lambda_s} - C, \quad (13)$$

at the left ( $L$ ) and right ( $R$ ) FM–SC interfaces. Thus we have six relations, i.e., Eqs. (8)–(13), which determine all the four constants ( $A$ – $D$ ) in the expression for the electrochemical potential split, and the two interfacial values of  $\beta^{L,R}$ . Once the interfacial quantities are known, the position dependence of  $\beta(x)$  throughout the trilayer can be found by considering Eqs. (8), (9), and (11), but this time evaluated at an arbitrary position  $x$ . Substituting  $\beta(x)$  in Eqs. (2a) and (2b) [i.e.,  $j_{\uparrow} = \beta(x)j$ ] and integrating, we then obtain the spatial dependence of electrochemical potentials of both spin types, i.e.,  $\mu_{\uparrow}(x)$  and  $\mu_{\downarrow}(x)$ . From the solutions, we obtain the interfacial

discontinuities in  $\mu$  at the FM–SC interfaces, i.e.,

$$\Delta\mu_{\uparrow}^0 = \frac{ej_c\beta^L}{G_{\uparrow\text{eq}}^L}, \quad (14)$$

$$\Delta\mu_{\downarrow}^0 = \frac{ej_c(1 - \beta^L)}{G_{\downarrow\text{eq}}^L}, \quad (15)$$

$$\Delta\mu_{\uparrow}^w = \frac{ej_c\beta^R}{G_{\uparrow\text{eq}}^R}, \quad (16)$$

$$\Delta\mu_{\downarrow}^w = \frac{ej_c(1 - \beta^R)}{G_{\downarrow\text{eq}}^R}, \quad (17)$$

Eqs. (14)–(17) follow directly from Eq. (3). Note, that we have assumed initial arbitrary values for the interfacial conductances  $G_{\uparrow(\downarrow)}^{L,R}$ . In actual fact,  $G_{\uparrow(\downarrow)}^{L,R}$  depends on the barrier height and profile at the FM–SC interfaces, as well as the potential discontinuity  $\Delta\mu_{\uparrow(\downarrow)}^{L,R}$  across the interfaces. Due to the dependence of  $G_{\uparrow(\downarrow)}^{L,R}$  on  $\Delta\mu_{\uparrow(\downarrow)}^{L,R}$ , a self-consistency loop is formed in which  $\Delta\mu_{\uparrow(\downarrow)}^{L,R}$  of Eqs. (14)–(17), which are determined by the DD model, is fed into the ballistic model to evaluate  $G_{\uparrow(\downarrow)}^{L,R}$ .

The ballistic tunneling model to evaluate  $G_{\uparrow(\downarrow)}^{L,R}$  is illustrated schematically in Fig. 1. The potential  $\mu$  is drawn only for the majority spin and a similar one can be drawn for the minority spin. For simplicity, the barrier profile is assumed to be delta functions with spin-differential heights, i.e.,  $U_{\uparrow(\downarrow)}^L\delta(x) + U_{\uparrow(\downarrow)}^R\delta(x-w)$ . We also assume symmetry of the two FM–SC junctions, so that the barrier height is the same for both left and right interfaces, i.e.,  $U_{\uparrow(\downarrow)}^L = U_{\uparrow(\downarrow)}^R$ . Both FM layers are taken to be semi-infinite.  $E_B$  is the shift in 2DEG Fermi level so as to align it with the Fermi level of the FM layers, i.e.,  $E_B = E_F(\text{Fe}) - E_F(2\text{DEG})$ . The Fermi-wave vectors at  $x = 0^{\pm}$  and  $x = w^{\pm}$  can, respectively, be written as

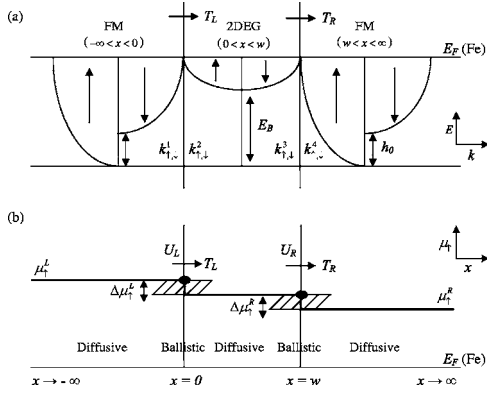


FIG. 1. (a) Schematic  $(E, k)$  band-diagram of FM-2DEG-FM trilayer. In the FM contacts, the conduction band edge is shifted by  $h_0$  (molecular field) for the minority spin carriers. Also shown are  $k_{1,2}$  and  $k_{3,4}$  which are the wavevectors at  $x=0^{\pm}$  and  $x=w^{\pm}$  respectively. (b) Position dependence of  $\mu_{\uparrow}$  for the three parts of the structure. Also shown are the discontinuities in  $\mu_{\uparrow}$  due to interfacial resistance. The hatched regions indicate the regions where we have considered ballistic transport i.e. only in the vicinity of interface. A similar diagram can also be drawn for  $\mu_{\downarrow}$ . Note that for simplicity we have not drawn the slope of the electrochemical potential in the figure.

$$k_{\uparrow}^1 = \sqrt{\frac{2m_{\text{Fe}}^*(E_{\text{F}}^{\text{Fe}} + \delta\mu_{\uparrow}^{1,n.l.})}{\hbar^2}}, \quad (18a)$$

$$k_{\downarrow}^1 = \sqrt{\frac{2m_{\text{Fe}}^*(E_{\text{F}}^{\text{Fe}} + \delta\mu_{\downarrow}^{1,n.l.} - h_0)}{\hbar^2}}, \quad (18b)$$

$$k_{\uparrow}^2 = \sqrt{\frac{2m_{\text{GaAs}}^*(E_{\text{F}}^{\text{Fe}} + \Delta\mu_{\uparrow}^0 + \delta\mu_{\uparrow}^{2,n.l.} - E_B)}{\hbar^2}}, \quad (19a)$$

$$k_{\downarrow}^2 = \sqrt{\frac{2m_{\text{GaAs}}^*(E_{\text{F}}^{\text{Fe}} + \Delta\mu_{\downarrow}^0 + \delta\mu_{\downarrow}^{2,n.l.} - E_B)}{\hbar^2}}, \quad (19b)$$

$$k_{\uparrow}^3 = \sqrt{\frac{2m_{\text{GaAs}}^*(E_{\text{F}}^{\text{GaAs}} + \delta\mu_{\uparrow}^{3,n.l.})}{\hbar^2}}, \quad (20a)$$

$$k_{\downarrow}^3 = \sqrt{\frac{2m_{\text{GaAs}}^*(E_{\text{F}}^{\text{GaAs}} + \delta\mu_{\downarrow}^{3,n.l.})}{\hbar^2}}, \quad (20b)$$

$$k_{\uparrow}^4 = \sqrt{\frac{2m_{\text{Fe}}^*(E_{\text{F}}^{\text{Fe}} + \Delta\mu_{\uparrow}^w + \delta\mu_{\uparrow}^{4,n.l.})}{\hbar^2}}, \quad (21a)$$

$$k_{\downarrow}^4 = \sqrt{\frac{2m_{\text{Fe}}^*(E_{\text{F}}^{\text{Fe}} - h_0 + \Delta\mu_{\downarrow}^w + \delta\mu_{\downarrow}^{4,n.l.})}{\hbar^2}}, \quad (21b)$$

where  $\delta\mu_{\uparrow,\downarrow}^{n.l.}$  represents the nonlinear (non-Ohmic) part of electrochemical potential  $\mu$  in the vicinity of both interfaces, due to spin accumulation. By flux and wave function matching at the interfaces, the transmission coefficients across the interfaces are given by

$$T_{\uparrow,\downarrow}^L = \frac{v_{\uparrow,\downarrow}^{L,\text{GaAs}}}{v_{\uparrow,\downarrow}^{L,\text{Fe}}} \left| \frac{2v_{\uparrow,\downarrow}^{L,\text{Fe}}}{v_{\uparrow,\downarrow}^{L,\text{Fe}} + v_{\uparrow,\downarrow}^{L,\text{GaAs}} - 2U_{\uparrow,\downarrow}^L \delta t / i\hbar} \right|^2, \quad (22)$$

$$T_{\uparrow,\downarrow}^R = \frac{v_{\uparrow,\downarrow}^{R,\text{Fe}}}{v_{\uparrow,\downarrow}^{R,\text{GaAs}}} \left| \frac{2v_{\uparrow,\downarrow}^{R,\text{GaAs}}}{v_{\uparrow,\downarrow}^{R,\text{GaAs}} + v_{\uparrow,\downarrow}^{R,\text{Fe}} - 2U_{\uparrow,\downarrow}^R \delta t / i\hbar} \right|^2, \quad (23)$$

where  $v_{\uparrow,\downarrow}^{L(\text{R})\text{Fe}} = \hbar k_{\uparrow,\downarrow}^{1(4)} / m_{\text{Fe}}^*$  and  $v_{\uparrow,\downarrow}^{L(\text{R})\text{GaAs}} = \hbar k_{\uparrow,\downarrow}^{2(3)} / m_{\text{GaAs}}^*$ . We have used velocities instead of  $k$  vectors in the expressions for  $T_{\uparrow,\downarrow}^{L,R}$  to simplify the expressions.  $\delta t$  is the thickness of the tunnel barrier which is taken to be thin (1 nm) in order to achieve good spin-tunneling properties.<sup>18–20</sup> The prefactors  $v_{\uparrow,\downarrow}^{L,\text{GaAs}} / v_{\uparrow,\downarrow}^{L,\text{Fe}}$  and  $v_{\uparrow,\downarrow}^{R,\text{Fe}} / v_{\uparrow,\downarrow}^{R,\text{GaAs}}$  of Eqs. (22) and (23), respectively, ensure flux continuity across the two FM–SC interfaces. The interfacial resistance  $R_{\uparrow,\downarrow}$  is then given by

$$\frac{1}{R_{\uparrow,\downarrow}^{L,R}} = G_{\uparrow,\downarrow}^{L,R} = \frac{e^2}{h} T_{\uparrow,\downarrow}^{L,R} n_m. \quad (24)$$

The above is obtained from Landauer's formula, where  $n_m$  is the number of transverse modes. To simplify self-consistent determination of interface resistance, we restrict our analysis to one transverse conductance mode only ( $n_m=1$ ). This may be achieved, e.g., by constricting the FM–SC interface to a narrow channel, so that it acts as a mode filter, and allows only one transverse mode to pass through.

A self-consistency loop linking  $G_{\uparrow,\downarrow}^{L,R}$  on  $\Delta\mu_{\uparrow,\downarrow}^{L,R}$  can be formed by considering the DD results of Eqs. (14)–(17), and the ballistic model results of Eqs. (18)–(24). The self-consistency loop is terminated when the values of  $G_{\uparrow,\downarrow}^{L,R}$  has converged to better than 0.1% accuracy. Table I lists all the parameter values assumed in the numerical calculations.

### III. RESULTS AND DISCUSSION

#### A. Interfacial resistance and analysis of tunnel barrier

Interfacial resistance is a vital requirement for efficient spin injection and magnetoresistive effect in hybrid trilayer structures.<sup>21</sup> We first analyzed the interfacial resistance at the left and right interface in our structure and found that the two are asymmetric with respect to each other. To explain this, we note that from Eqs. (22) and (23), the transmission probability  $T$  depends on the respective  $\mathbf{k}$ -vectors at the FM and SC sides of the interface. These are given by Eqs. (18)–(21), from which we infer that the asymmetry in  $T$  is due to (i) the interfacial discontinuity in potential  $\Delta\mu_{\uparrow(\downarrow)}^{L,R}$ , and (ii) the nonlinear part of electrochemical potentials  $\delta\mu_{\uparrow,\downarrow}^{n.l.}$  which corresponds to spin accumulation. Both these effects arise when a finite current flows across the structure (i.e., when a finite bias voltage is applied). The discontinuity in electrochemical potentials at the two interfaces  $\Delta\mu_{\uparrow,\downarrow}^{L,R}$  is caused by the presence of interfacial resistances and has been obtained self-consistently in our model. We define the percentage asymmetry  $A_s$ , in interfacial resistances as:

$$A_s = \left( 1 - \frac{R_L}{R_R} \right) \times 100, \quad (25)$$

$R_L$  and  $R_R$  are the mean values of interfacial resistances experienced by up and down spin electrons, and are expressed

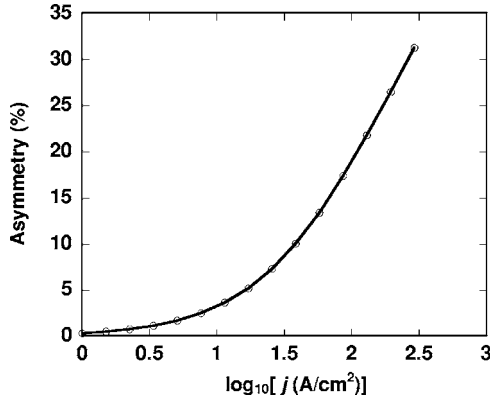


FIG. 2. Plot of asymmetry  $A_s$  [as defined in Eq. (25)] in interfacial resistance as a function of current density  $j$ .

as resistance-area products (i.e., in terms of  $1/G_{\text{eq}}$ ). In Fig. 2, we plot the asymmetry  $A_s$  as a function of bias current density. As the bias current increases from 1 to  $10^3$  A/cm<sup>2</sup>, the asymmetry in interfacial resistances increases from almost 0 to over 30%. This figure illustrates that the degree of asymmetry  $A_s$  is determined by the applied bias voltage and hence current density across the tunneling barriers, which in turn determines the size of the discontinuity in the electrochemical potential and spin accumulation at the two interfaces. Both of these contribute to the observed asymmetry. It can also be inferred that  $A_s$  changes sign (i.e., with  $R_L$  being larger than  $R_R$ ) when the current direction is reversed.

In Fig. 3, we have plotted  $R_L$  as the resistance-area product taking different values of 2DEG GaAs Fermi levels at  $U_{\uparrow(\downarrow)}=500$  (250) meV. This figure shows that when we increase the doping density in the SC layer, i.e., increase the Fermi level within the conduction band, the interface resistance decreases. This trend may be explained by examining Eq. (22) that as  $E_F$  of 2DEG increases  $T_L$  increases and hence  $R_L$  decreases (n.b.  $E_F^{\text{Fe}} \gg E_F^{\text{GaAs}}$ ). A similar trend also applies to  $R_R$ . The value of interfacial resistance  $R_L$  at  $E_F$  of 2DEG GaAs=3.5 meV as obtained from our model is  $5.66 \times 10^{-5} \Omega \text{ cm}^2$ . This value is about 2 orders of magnitude higher than the value of interfacial resistance assumed by Yu and Flatté<sup>11</sup> and thus should improve the low ( $\sim 0.01$ ) spin-injection efficiency of their structure.

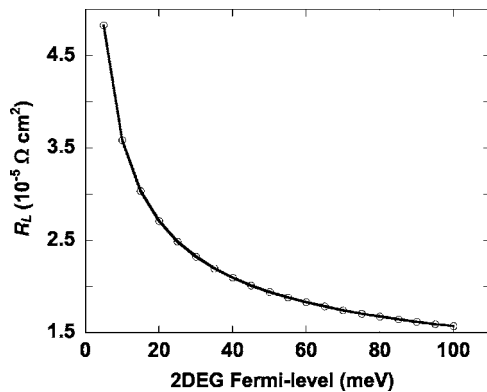


FIG. 3. Plot of the interfacial resistance  $R_L$  vs 2DEG Fermi level.

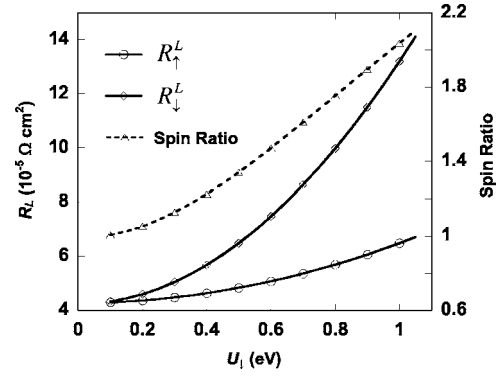


FIG. 4.  $R_L$  for both spins vs increasing tunnel barrier strengths of  $U_{\downarrow}$  barrier keeping  $U_{\uparrow}/U_{\downarrow}$  fixed at 0.5. Dotted curve shows the spin-ratio  $R_{\uparrow}^L/R_{\downarrow}^L$ .

It should also be noted that spin-dependent tunnel barriers  $U$  at two interfaces helps in maintaining the “spin-asymmetry” in  $R_L$  as well as  $R_R$  and thus contributes to spin polarization and magnetoresistance. At barrier heights of  $U_{\uparrow,\downarrow}=500$  (250) meV, the spin polarization of  $R_L$  at left and right interfaces  $(\Delta R/R)_{L,R}=(R_{\downarrow}^{L,R}-R_{\uparrow}^{L,R})/(R_{\downarrow}^{L,R}+R_{\uparrow}^{L,R})$  is found to vary in a short range from 10% to 15%, and thus remains fairly constant with 2DEG Fermi level. To enhance this ratio and hence the spin injection efficiency, we need to study the effect of different barrier heights  $U_{\uparrow,\downarrow}$  on the spin-asymmetry of  $R_L$ . In Fig. 4,  $R_{\uparrow,\downarrow}^L$  at left interface and the ratio  $(R_{\uparrow}^L/R_{\downarrow}^L)$  are plotted for different  $U_{\uparrow}$  and  $U_{\downarrow}$ , while keeping their relative ratio  $(U_{\uparrow}/U_{\downarrow})$  constant at 0.5, and  $E_F$  of the 2DEG fixed at 3.5 meV. The magnitude of both  $R_{\uparrow}^L$  and  $R_{\downarrow}^L$  increase with barrier height  $U$ , and more significantly, so does the spin asymmetry in  $R_L$ . The latter trend is due to the spin asymmetry of  $U$  adding to that of the  $k$ -wave vectors [see Eqs. (22) and (23)], resulting in an increase in the overall spin asymmetry of the transmission probability  $T$  and thus  $R_L$ . The spin asymmetry of  $R_L$  translates into a large increase in the spin-injection efficiency from  $<1\%$  at  $U_{\downarrow}=0.1$  eV to about 25% at  $U_{\downarrow}=1$  eV, keeping  $U_{\uparrow}=0.5U_{\downarrow}$  (Fig. 5). As expected, the spin-injection efficiency can be further enhanced

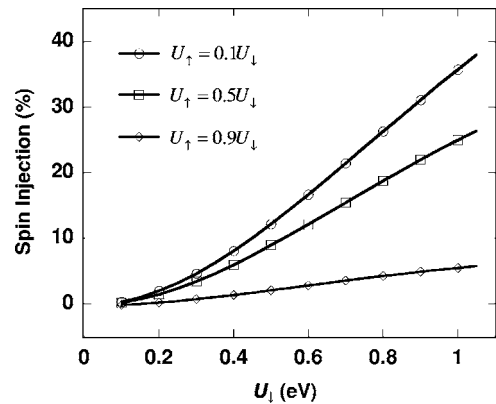


FIG. 5. Spin-injection vs tunnel barrier strengths of  $U_{\downarrow}$  barrier for different ratios of  $U_{\uparrow}/U_{\downarrow}$  thus showing the effect of varying height and spin asymmetry of tunnel barriers on the spin-injection efficiency.

to 40% by increasing the spin asymmetry in  $U$  as can be seen from Fig. 5.

### B. Magnetoresistance

Finally, we consider the magnetoresistance (MR) ratio of the trilayer structure, i.e., the resistance change when the magnetization of the FM contacts switches from parallel ( $P$ ) to antiparallel ( $AP$ ) alignment. In calculating the MR ratio, the thickness of the FM contacts are taken to be equal to their spin-diffusion length  $\lambda_{sd}$ , since the spin dependence of current in the FM contacts primarily occurs within  $\lambda_{sd}$  from the FM–SC interface. Note, that the two-current model, e.g., of Schmidt *et al.*<sup>9</sup> is not applicable to our case, since by assuming a finite spin diffusion length, we have introduced a coupling between the two spin currents within the SC.

In our analysis, we have assumed a constant current across the device, so that the MR can be expressed as

$$\frac{\Delta R}{R} = \frac{R_{AP} - R_P}{R_{AP}} = \frac{\Delta\mu_0^{AP} - \Delta\mu_0^P}{\Delta\mu_0^{AP}}, \quad (26)$$

where

$$\Delta\mu_0^{P,AP} = \mu_0^{P,AP}(x = -\lambda_{FM}) - \mu_0^{P,AP}(x = w + \lambda_{FM}), \quad (27)$$

where,  $\mu_0$  is the linear spin-independent component of the electrochemical potential  $\mu_{\uparrow,\downarrow}(x)$ , which is solely due to the applied voltage drop across the device.

We first discuss the MR ratio in FM/SC/FM structures, i.e., without the  $U$  barriers at the interface. In the absence of any tunnel barrier at the interface, i.e., zero interfacial resistance, a negligible MR effect is obtained. It has been shown by Schmidt *et al.*<sup>9</sup> in their diffusive calculations that  $\Delta R/R$  is less than  $10^{-7}$  without any interfacial tunnel barrier. It is only at FM contact polarization  $\alpha_c$  close to 0.99 that MR approaches 0.1%, but this is still far too low for any practical realization of spintronics devices. Schmidt *et al.* have attributed such small MR values to the conductivity mismatch between FM and SC. Hence, to achieve high MR ratio in a FM–SC–FM trilayer, we require either a highly spin-asymmetric  $R_I$  with a large magnitude so that its resistive contribution far exceeds that of the SC layer, or a very high contact spin polarization which approaches ideal half-metallic value of 100%. Experimentally also, Motsnyi *et al.*<sup>18</sup> have achieved large values of MR of about 28% only when they consider very large interfacial resistance of the order of  $10^{-3} \Omega \text{ cm}^2$ .

Next, we analyze the case of a NM/SC/NM structure (where NM is a nonmagnetic metal contact) with spin-dependent tunnel barrier  $U$  at the NM–SC interface. The numerical results for this configuration are virtually identical to that of a FM/SC/FM structure, which will be presented later. This is because the overall spin transport is largely determined by the spin-filtering effects of the tunnel barriers and not the spin polarization of the contacts. Thus, there is very little difference in the spin injection efficiency and MR when we exchange the ferromagnetic contacts with nonmagnetic ones. Numerically, we calculate the MR ratio for the case of nonmagnetic contacts ( $\alpha_c=50\%$ ) and compare it with the

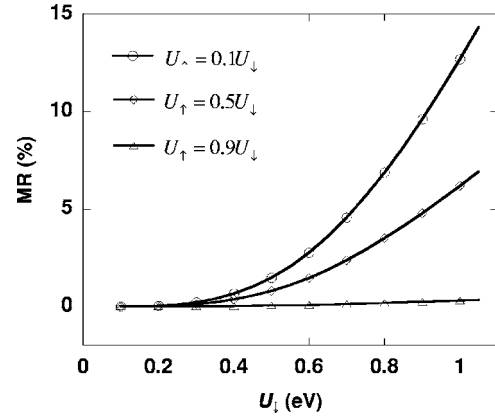


FIG. 6. MR vs tunnel barrier strengths of  $U_{\perp}$  barrier for different ratios of  $U_{\uparrow}/U_{\downarrow}$  thus showing the effect of varying height and spin asymmetry of tunnel barriers on the MR ratio.

case of FM contacts ( $\alpha_c=70\%$ ), with a small tunnel barrier spin asymmetry of  $U_{\uparrow}=0.9U_{\downarrow}$ . We find a difference in MR of the order of 0.1% when  $U_{\perp}=100$  meV. The difference is further reduced when (i) a larger barrier height is used (e.g., for  $U_{\perp}=1$  eV, the difference is a negligible  $10^{-4}\%$ ) and (ii) when the spin asymmetry of  $U$  is increased. This is because both these factors will increase the dominance of the interfacial tunnel barriers over the contact polarization, in determining the overall spin transport.

Finally, we analyze the MR effect in a FM/SC/FM structure with spin-dependent tunnel barriers at the interface. As can be seen from Fig. 6, taking the  $E_F$  of 2DEG GaAs to be 3.5 meV, and the barrier height  $U_{\downarrow(\uparrow)}=500$  (250) meV, the MR ratio is found to be close to 1% which is much lower than the spin polarization of  $U$ . But increasing the barrier height to 1 eV, considering the largest spin-asymmetry (i.e.,  $U_{\uparrow}=0.1U_{\downarrow}$ ) in Fig. 6, the MR ratio can go up to about 15%. To explain this, we note that the resistance  $R_L$  of  $8.78 \times 10^{-5} \Omega \text{ cm}^2$  at  $U_{\perp}=1$  eV with  $U_{\uparrow}=0.1U_{\downarrow}$ , i.e., highest spin-asymmetry considered, is higher than  $1.81 \times 10^{-6} \Omega \text{ cm}^2$  which is the resistance of 2DEG layer (taking the 2DEG resistivity to be  $0.18 \Omega \text{ cm}$ , corresponding to the doping of  $10^{16} \text{ cm}^{-3}$ ). To increase the MR ratio, we require the spin-dependent interfacial resistances to be comparable to the spin-independent resistance of the SC (2DEG) layer, as suggested in Ref. 10. Earlier, we showed that the resistance  $R_R$  associated with transmission from SC to FM layer, is larger than  $R_L$  due to the asymmetry ( $A_s$ ). Our finding indicates that to enhance the MR ratio, it is more effective to focus on the magnitude and spin asymmetry of the SC to FM interfacial resistance of the trilayer.

### IV. CONCLUSION

We have presented a self-consistent transport model to calculate the interfacial resistance ( $R_I$ ) values in a FM–SC–FM trilayer structure in which the SC layer is modeled as a highly doped  $n^{++}$  AlGaAs–GaAs 2DEG while the interfacial resistance at the FM–SC junction is modeled as delta potential ( $\delta$ ) barriers. The self-consistent scheme con-

nects the drift-diffusion model used for evaluating the spin-split and interfacial discontinuity in the electrochemical potential, and the ballistic model to determine the transmission coefficient and hence interfacial resistance at the two FM-SC interfaces. The self-consistent values of  $R_I$  are then used to calculate spin injection and MR ratio of the trilayer structure. We observed that the values of  $R_I$  at left and right interfaces are asymmetric with respect to each other, and this asymmetry increases with the applied bias voltage. A high  $R_I$  and a high spin asymmetry in the interfacial barrier are required to achieve high spin injection efficiency, which is a principal requirement in a semiconductor spintronics device. This may be achieved in practice by introducing tunnel barriers at the FM-SC interface, which are naturally spin asymmetric due to the different band structures in the FM layers for minority

and majority spins. The requirements are even more stringent for achieving significant MR effect. One requires an even larger  $R_I$  (which provides a resistance comparable to that of the SC layer) and an almost 100% spin polarized tunnel barrier to achieve appreciable magnetoresistive effect.

#### ACKNOWLEDGMENTS

The authors would like to thank the National University of Singapore (R-263-000-329-112) and the Agency for Science, Technology and Research (A\*STAR) of Singapore (Grant No. 022 105 0053) for financially supporting the work. One of the authors (S. A.) would like to thank NUS for his research scholarship.

- 
- <sup>1</sup>S. A. Wolf, D. D. Awschalom, R. A. Buhrman, J. M. Daughton, S. von Molnar, M. L. Roukes, A. Y. Chtchelkanova, and D. M. Treger, *Science* **294**, 1488 (2001).
- <sup>2</sup>J. M. Kikkawa and D. D. Awschalom, *Nature (London)* **397**, 139 (1999).
- <sup>3</sup>J. Nitta, T. Akazaki, H. Takayanagi, and T. Enoki, *Phys. Rev. Lett.* **78**, 1335 (1997).
- <sup>4</sup>S. Datta and B. Das, *Appl. Phys. Lett.* **56**, 665 (1990).
- <sup>5</sup>P. R. Hammar, B. R. Bennett, M. J. Yang, and M. Johnson, *Phys. Rev. Lett.* **83**, 203 (1999).
- <sup>6</sup>S. Gardelis, C. G. Smith, C. H. W. Barnes, E. H. Linfield, and D. A. Ritchie, *Phys. Rev. B* **60**, 7764 (1999).
- <sup>7</sup>A. T. Hanbicki, O. M. J. van't Erve, R. Magno, G. Kioseoglou, C. H. Li, B. T. Jonker, G. Itskos, R. Mallory, M. Yasar, and A. Petrou, *Appl. Phys. Lett.* **82**, 4092 (2003).
- <sup>8</sup>P. C. van Son, H. van Kempen, and P. Wyder, *Phys. Rev. Lett.* **58**, 2271 (1987).
- <sup>9</sup>G. Schmidt, D. Ferrand, L. W. Molenkamp, A. T. Filip, and B. J. van Wees, *Phys. Rev. B* **62**, R4790 (2000).
- <sup>10</sup>E. I. Rashba, *Phys. Rev. B* **62**, R16267 (2000).
- <sup>11</sup>Z. G. Yu and M. E. Flatte, *Phys. Rev. B* **66**, 235302 (2002).
- <sup>12</sup>H. B. Heersche, Th. Schapers, J. Nitta, and H. Takayanagi, *Phys. Rev. B* **64**, 161307(R) (2001).
- <sup>13</sup>Y. C. Tao and D. Y. Xing, *J. Magn. Magn. Mater.* **251**, 163 (2002).
- <sup>14</sup>D. L. Smith and R. N. Silver, *Phys. Rev. B* **64**, 045323 (2001).
- <sup>15</sup>S. Zhang, P. M. Levy, and A. Fert, *Phys. Rev. Lett.* **88**, 236601 (2002).
- <sup>16</sup>M. D. Stiles and A. Zangwill, *J. Appl. Phys.* **91**, 6812 (2002).
- <sup>17</sup>I. L. Drichko, A. M. Diakonov, I. Yu. Smirnov, Yu. M. Galperin, and A. I. Toropov, *Phys. Rev. B* **62**, 7470 (2000).
- <sup>18</sup>V. F. Motsnyi, J. De Boeck, J. Das, W. Van Roy, G. Borghs, E. Goovaerts, and V. I. Safarov, *Appl. Phys. Lett.* **81**, 265 (2002).
- <sup>19</sup>Z. Li, C. de Groot, and J. H. Moodera, *Appl. Phys. Lett.* **77**, 3630 (2000).
- <sup>20</sup>M. Covington, J. Nowak, and D. Song, *Appl. Phys. Lett.* **76**, 3965 (2000).
- <sup>21</sup>S. Agrawal, M. B. A. Jalil, K. L. Teo, and Y. F. Liew, *J. Appl. Phys.* **97**, 103907 (2005).